Neutrophil-Derived Interleukin 16 in Premetastatic Lungs Promotes Breast Tumor Cell Seeding

Cancer Growth and Metastasis
Volume 10: 1–14

DOI: 10.1177/1179064417738513

Kim Donati[1,2], Christelle Sépult[1,2], Natacha Rocks[1,2], Silvia Blacher[1], Catherine Gérard[1,2], Agnès Noel[1] and Didier Cataldo[1,2]

[1]Laboratory of Tumor and Development Biology, Groupe Interdisciplinaire de Génoprotéomique Appliquée-Cancer (GIGA-Cancer), University of Liège, Liège, Belgium. [2]Laboratory of Pneumology, Groupe Interdisciplinaire de Génoprotéomique Appliquée-Cancer (GIGA-Cancer), University of Liège, Liège, Belgium.

ABSTRACT: The premetastatic niche in distant organs prior to metastatic cell arrival emerged as an important step in the metastatic cascade. However, molecular mechanisms underlying this process are still poorly understood. In particular, whether neutrophil recruitment at a premetastatic stage promotes or inhibits metastatic cell seeding has to be clarified. We aimed at unraveling how neutrophil infiltration in lung parenchyma induced by the distant primary tumor influences the establishment of lung metastasis. Elevated neutrophil counts and IL-16 levels were found in premetastatic lungs in a syngenic mouse model using 4T1 tumor cells. 4T1 cell–derived soluble factors stimulated IL-16 secretion by neutrophils. The functional contribution of IL-16 is supported by metastasis burden reduction in lungs observed on instillation of an IL-16 neutralizing antibody. Moreover, IL-16 promotes *in vitro* 4T1 cell adhesiveness, invasiveness, and migration. In conclusion, at a premetastatic stage, neutrophil-derived IL-16 favors tumor cell engraftment in lung parenchyma.

KEYWORDS: Tumor microenvironment, breast cancer, metastasis, lungs, neutrophils, IL-16

RECEIVED: April 4, 2017. **ACCEPTED:** September 4,2017.

PEER REVIEW: Three peer reviewers contributed to the peer review report. Reviewers' reports totaled 862 words, excluding any confidential comments to the academic editor.

TYPE: Original Research

FUNDING: The author(s) disclosed receipt of the following financial support for the research, authorship, and/or publication of this article: This study was financially supported by grants from the Fonds National pour la Recherche Scientifique (FRS-FNRS Télévie, grant no. 7463012F), the Centre AntiCancéreux (University of Liège), the Foundation against Cancer (foundation of public interest, Belgium), Interuniversity Attraction Poles Program-Belgian State-Belgian Science Policy-project P7/30, and the Fonds Léon Fredericq (University of Liège).

DECLARATION OF CONFLICTING INTERESTS: The author(s) declared the following potential conflicts of interest with respect to the research, authorship, and/or publication of this article: D.C. is the founder of Aquilon Pharmaceuticals, received speaker fees from AstraZeneca, Boehringer Ingelheim, Novartis, Mundipharma, Chiesi, GSK and received consultancy fees from AstraZeneca, Boehringer Ingelheim, and Novartis for the participation to advisory boards. None of these activities have any connection with oncology or development of drugs in the field of oncology.

CORRESPONDING AUTHOR: Didier Cataldo, Laboratory of Tumor and Development Biology, Groupe Interdisciplinaire de Génoprotéomique Appliquée-Cancer (GIGA-Cancer), University of Liège, Avenue Hippocrate 13, 4000 Liège, Belgium.
Email: didier.cataldo@ulg.ac.be

Introduction

Although cancer therapies are improving the past decades, 90% of patient mortality is the consequence of metastatic dissemination of the primary tumor.[1] In 2016, breast cancer was the most frequent malignant disease in women.[2] Although patients with breast cancer displaying metastasis at diagnosis displayed a poor survival rate of only 10% in the 5 years following the diagnosis in the 1970s, their survival rose to just over 40% in the 2000s.[3] A recent survey identified metastasis from breast cancer as a current challenge in patients with a median survival of 29.4 months when considering women with a metastatic disease at the time of diagnosis.[4]

It is now very well accepted that metastatic foci develop in specific secondary sites according to the primary tumor type. In 1889, Stephen Paget already reported the "seed and soil theory" suggesting that metastatic tumor cells will preferably disseminate in a specific target organ.[5] Lungs are a common site for the metastatic spread of breast cancer.[6] However, mechanisms supporting this observation need to be clarified but should aim attention at specific modifications of the microenvironment in the target organ. In the past decade, the development of a premetastatic niche in distant organs prior to metastatic cell arrival has been reported and cells and molecules contributing to the setup of this niche have been extensively characterized.[7–9] Myeloid progenitors were shown to be recruited in the target organ before ingression of metastatic tumor cells,[10,11] and growing number of studies support the key contribution of myeloid cells in the establishment of the premetastatic niche, which influences tumor cell engraftment.[12–18] Although neutrophil contribution to breast cancer metastases and premetastatic niche has been reported, their role is to date controversial, and the mechanisms involved remain poorly understood.[15–17]

Interleukine 16 (IL-16) was primarily identified as a key factor for lymphocyte recruitment and activation.[19] IL-16 precursor is intracellularly activated by a proteolytic cleavage before being secreted and is produced by a large variety of cells including T lymphocytes, mast cells, macrophages, eosinophils, dendritic cells, monocytes, fibroblasts, and bronchial epithelium.[20] Interestingly, neutrophils are also able to produce IL-16.[21] Interleukin 16 displays chemotactic properties by interacting with CD4 expressed by lymphocytes[22] and CD9 expressed by mast cells[23] and has been associated with different inflammatory diseases such as asthma, polyarthritis, lung emphysema, and Crohn disease.[24–30] Moreover, accumulating evidence suggests a key role for IL-16 in several primary cancers including multiple myeloma,[20,31] gastrointestinal,[32,33] ovarian,[34] prostate,[35,36] and breast cancers.[32] Elevated IL-16 levels were reported in serum samples of patients with breast cancer as compared with healthy subjects[32]. A proposed mechanism for its implication in tumorigenesis relates to its capacity to recruit macrophages to the primary tumor through its interaction with CD4.[37] However,

the potential role of IL-16 in the establishment of metastasis in distant organs is still unknown.

In this study, we aimed at investigating the mechanisms underlying the elaboration of a premetastatic niche in lungs prior to the arrival and engraftment of metastatic tumor cells. For this, we used a syngenic mouse model in which 4T1 mammary tumor cells were subcutaneously injected. 4T1 cells were chosen in this study because they metastasize to lungs and they induce a strong granulocytosis in the organs of immunocompetent mice, which are targets for metastatic seeding.[38] Based on our data, we could assign a novel function to IL-16 in the neutrophil-driven lung remodeling that contributes to metastatic cell colonization.

Materials and Methods

Cell cultures

Murine 4T1 mammary tumor cells expressing luciferase (clone 1A1; Xenogen Corporation, Almeda, CA, USA) and murine endothelial SVEC4.10 cells (ATCC, USA) were cultured in Dulbecco's Modified Eagle's medium (DMEM) (Thermo Fisher Scientific, Waltham, MA, USA) supplemented with 10% fetal bovine serum (FBS), 1% penicillin/streptomycin, and 1% L-glutamine.

Animals and experimental tumor xenograft model

The experimental protocol for animal studies was approved by the Ethical Committee of the University of Liege. Male 6- to 8-week-old Balb/c mice (Janvier Labs, Le Genest-Saint-Isle, France) were subcutaneously injected in each flank with 2×10^5 4T1 cells. Mice were killed 3, 7, 9, 14, and 21 days after tumor cell injection. After killing, the presence of 4T1 cells in lungs was monitored using Xenogen IVIS 200 (Perkin Elmer, Waltham, MA, USA). Analysis and quantification of luciferase activity (counts) were performed with the Life Image 4.4 software (Perkin Elmer).

BAL, lung tissue sampling, and protein extraction

After killing, a cannula was inserted in the trachea and a BAL was manually performed by injecting 4 × 1 mL of phosphate-buffered saline (PBS)-EDTA 0.05 mM (Calbiochem, Schwalbach, Germany) in lungs. Recovered BAL was centrifuged (282*g* for 10 minutes, at 4°C) and supernatants (bronchoalveolar fluids or BALF) were frozen at −80°C for future analyses, whereas cell pellets were cytocentrifuged and stained with Diff-Quik (Dade, Brussels, Belgium). Differential cell counts were achieved based on morphological criteria.

After BAL collection, the right lung was clamped, harvested, and snap-frozen in liquid nitrogen. The left lung was insufflated with 4% paraformaldehyde and embedded in paraffin for histologic analysis.

For total protein extraction, lung tissues were homogenized using a Mikro-Dismembrator device (Braun Biotech International, Melsungen, Germany). Crushed lungs were incubated overnight at 4°C in a solution containing 2 M urea, 1 M NaCl, and 50 mM Tris (pH 7.5). Samples were then centrifuged for 15 minutes at 13 000*g*, and supernatants were collected for protein assessments.

Lung primary cultures

After killing, lungs were collected, manually chopped, and digested for 1 hour at 37°C in DMEM medium containing 1-mg/mL collagenase clostridium histolyticum (Sigma, Steinheim, Germany), Hanks buffer salt solution (Sigma), and 1% MEM Amino Acids (PromoCell, Heidelberg, Germany). Samples were centrifuged at 282*g* for 10 minutes at 4°C, and pellets were cultured in DMEM supplemented with 10% FBS, 1% amino acids, 5 µg/mL amphotericin B (Sigma), 0.5% gentamycin (Sigma), and 1% L-glutamine. Tumor cell colonies were visualized with Xenogen IVIS 200 after 4 to 6 days.

Premetastatic niche characteristic analysis

Collagen cross-linking was studied with a picro-red sirius staining. For this, slides were rehydrated and stained for 1 hour with a saturated aqueous solution of picric acid containing 10% Red 80 (Sigma). Slides were washed twice with a 0.5% acetic acid solution and dehydrated in 100% ethanol. Then, after a bath of xylene, slides were mounted. Cross-linked collagen fibers were visualized under a polarized light in optical microscopy. Quantification was performed using ImageJ software (5 blood vessels/slide, 5 sections/mouse). Results were expressed as the ratio between cross-linked collagen area and the perimeter of the corresponding blood vessel.

Expression of lysyl oxidase was analyzed by reverse transcription-polymerase chain reaction using GeneAmp Thermostable rTth Reverse Transcriptase RNA PCR kit (Perkin Elmer). Oligonucleotides were obtained from Eurogentec (Seraing, Belgium) and were designed according to the sequence available in the GenBank: 5′-TCCTCCAGACAGAAGCTTGCTT-3′ (antisense) and 5′-TGCCTGGCCAGTTCAGCATATA-3′ (sense). The sequence specificity was verified using NCBI BLASTN program (http://www.ncbi.nlm.nih.gov/BLAST/). Retrotranscription was performed on 4-ng total RNA samples at 70°C for 15 minutes. Polymerase chain reaction steps consisted of 94°C for 15 seconds, 60° for 20 seconds, and 72°C for 10 seconds during 38 cycles followed by 2 minutes at 72°C. Samples were migrated on a polyacrylamide gel and stained with GelStar (Biowhittaker, Indianapolis, IN, USA). Intensity of bands was quantified using Quantity One software (Bio-Rad, Hercules, CA, USA).

Analysis of gelatinase production and activity in the lungs was achieved by zymography as previously described.[39]

Chemokine array and ELISA

Chemokine array (R&D Systems, Wiesbaden, Germany) was performed according to the supplier's protocol. Membranes were first incubated with samples (pooled lung protein extracts,

n = 5) followed by a cocktail of biotin-labeled antibodies. Membranes were then incubated with streptavidin conjugated to horseradish peroxidase (HRP), and spots were detected with an ECL detection kit (Perkin Elmer).

IL-16 detection in lungs, serum samples, and BALF and detection of s100A8, KC, and GM-CSF in 4T1-conditioned medium were performed with respective Mouse DuoSet ELISA kits (R&D Systems) according to the manufacturer's protocol.

Western blotting

Pooled protein extracts (n = 10) were separated using a 16% polyacrylamide gel and transferred on a polyvinylidene fluoride membrane (Perkin Elmer), which was then blocked with a solution of PBS containing 10% dry milk and 0.1% Tween 20. A rabbit polyclonal anti-IL-16 (Santa Cruz, Santa Cruz, CA, USA) was applied on membranes overnight at 4°C. Membranes were washed and incubated with a swine anti-rabbit antibody conjugated to HRP (Dako, Glostrup, Denmark) for 1 hour at room temperature. ECL detection kit and LAS 4000 (Fuji Photo Film Co., Tokyo, Japan) allowed the detection of interest bands. Blots were reprobed with a rabbit anti-β-actin antibody (Sigma) as a loading control.

Immunological analysis

For IL-16 detection by immunohistochemistry, sections were rehydrated and heated in target retrieval buffer (Dako). Sections were rehydrated and heated in target retrieval buffer (Dako). Slides were then pretreated with 3% H_2O_2, blocked with 10% bovine serum albumin (BSA) and incubated with a rabbit polyclonal antibody targeted against mouse IL-16 (Santa Cruz) for 1 hour at room temperature. Slides were washed with 1% BSA. Sections were washed and incubated with an Envision goat anti-rabbit antibody (Dako). After final rinsing, 3,3′-diaminobenzidine (Dako) was added. Slides were washed, dried, and mounted.

For the co-detection of neutrophils and IL-16, immunofluorescence experiments were performed. Briefly, sections were rehydrated and heated in target retrieval buffer (Dako). After a bath overnight at 4°C in water, slides were blocked with 10% BSA and incubated 1 hour with a rabbit anti-mouse IL-16 (Santa Cruz) at room temperature. Then, slides were treated with a biotinylated polyclonal goat anti-rabbit (Dako) before a treatment with streptavidin conjugated to Alexa Fluor 555 (Invitrogen, Waltham, MA, USA). To detect neutrophils, slides were treated with rat anti-mouse neutrophils (NIMP-R14; Thermo Fisher Scientific) and then a goat anti-rat conjugated to Alexa Fluor 488 (Invitrogen). For nucleus detection, slides were mounted using DAPI Fluoromount-G (SouthernBiotech, Birmingham, AL, USA).

Conditioned medium administration and intravenous injection of 4T1 cells

Mice received a daily intratracheal instillation of conditioned medium during 7 days before being killed. Conditioned medium was obtained from 4T1 cell cultures incubated for 48 hours in serum-free and phenol-free DMEM. Cell viability after incubation was evaluated with trypan blue staining method. For experimental metastasis model, mice were injected with 10^5 tumor cells in the tail vein on day 3 after starting conditioned medium treatment.

Neutrophil isolation and depletion

To isolate neutrophils from lungs of tumor-bearing mice, lungs were collected after killing, manually chopped, and then digested with collagenase type IV (Life Technologies, Camarillo, CA, USA). Granulocytes were isolated using histopaque (Sigma) according to the supplier's protocol. Neutrophils were isolated from recovered cells using a MACS neutrophil isolation kit (Miltenyi Biotec, Bergisch Gladbach, Germany) according to the manufacturer's protocol. Purity of cell isolation was verified by cytocentrifugation and cytometry analysis using a V450-conjugated anti-mouse CD45 (BD Biosciences, San Jose, CA, USA), a PerCp Cy5.5-conjugated anti-mouse Gr1 (BD Biosciences), and a PE-conjugated anti-mouse CD11b (BD Biosciences).

The effect of a neutrophil depletion was analyzed using a blocking antibody. Tumor-bearing mice were intraperitoneally injected twice a week with either 100 µg antibody targeting Ly6G (clone 1A8) or rat IgG2a κ (BioLegend, San Diego, CA, USA) and were killed on day 7.

IL-16 neutralization by antibody treatment

At days 7, 11, 15, and 19 after tumor cell injection, tumor-bearing mice were intratracheally instilled with 50-µg/mL IL-16 blocking antibody. As mouse IL-16 shows more than 80% homology with the human form and consistent with previous reports,[40–42] we used a mouse-neutralizing anti-human IL-16 antibody (14.1) (BD Biosciences) to inhibit IL-16 in our experimental mouse model. Control mice were injected with corresponding concentrations of an IgG2A κ control isotype antibody (BD Biosciences). Mice were killed 48 hours after the last instillation.

Computerized quantification of lung tumor area

Slides stained with hematoxylin-eosin were scanned using the NanoZoomer 2.0-HT system (Hamamatsu, Corbais, Belgium). Images were registered in a Red Green Blue (RGB) format. Tumors and tissue were visualized as dark and light purple, respectively. Image analysis algorithm was implemented to automatically perform image processing and measurements using the image analysis toolbox of MATLAB 8.3 (R2014a) software (MathWorks Inc., Natick, MA, USA). To increase the contrast between stained regions and the surrounding tissue, the color excess transformation for the 3 RGB bands (ie, 2 times each band minus the 2 other bands) was applied to raw images. Tumors appear contrasted in blue component images. Binary

images of tumors were determined using a fixed threshold. To obtain the binary image of the tissue, the blue component was smoothed using a low-pass filter and then the resulting image binarized automatically. Binary images were finally used to determine the tumor density, defined as the number of pixels belonging from the tumor (tumor area) divided by the number of pixels belonging from the whole tissue (tissue area).

Proliferation assay

Proliferation in the presence of increasing concentration of a recombinant mouse IL-16 (Cell Guidance Systems Ltd, Babraham, Cambridge, UK) was evaluated using cell proliferation ELISA BrdU colorimetric kit (Roche, Mannheim, Germany) according to the supplier's protocol.

Boyden and invasion assays

IL-16 capacity to induce tumor cell attraction was studied using Boyden chamber's assay. Briefly, a cell suspension in serum-free medium is deposited in the upper compartment of inserts with a pore sire of 8 µm (Costar Corning, NY, USA). Serum-free medium containing increasing mouse recombinant IL-16 concentrations were added in the lower compartment. After 8 hours of cell migration, inserts were washed, fixed with methanol at −20°C during 30 minutes, dried, and stained with 4% Giemsa. Cells remaining in the upper compartment were eliminated with a cotton swab and membranes were mounted on a slide.

To analyze 4T1 cell invasion, a modified Boyden chamber's assay was achieved. Briefly, inserts were coated with Matrigel prepared previously as described before[43] and 4T1 cells were added in the upper insert compartment with several concentrations of IL-16, whereas the lower compartment was filled with standard complemented medium supplemented with 10% FBS. Cells were allowed to migration for 24 hours, the assay was finished following the protocol of a classical Boyden chamber's assay as described before.

Adhesion assay

4T1 cells were stained with a *CellTracker Green* CMFDA (Invitrogen) and 5×10^4 tumor cells were added on a confluent SVEC4.10 endothelial cell monolayer cultivated on a cover blade. After 45 minutes incubation in the presence of increased concentrations of recombinant IL-16, nonadherent 4T1 cells were eliminated and cover blades were mounted with DAPI Fluoromount-G (SouthernBiotech). Adherent green 4T1 cells were counted in 10 to 15 fields (20× magnification).

Scratch assay

4T1 cells were cultured to 100% confluence, then a wound was performed with the tip of a tip, and the plate was washed with PBS. Serum-free medium was added containing or not increasing concentrations of mouse recombinant IL-16. Proliferation of cells was inhibited by addition of cytosine β-D-arabinofuranoside hydrochloride (Sigma). The percentage of wound closure was calculated after 6 and 24 hours using the NIS-Elements Advanced Research software (Nikon Instruments Europe B.V., Amsterdam, Netherlands).

Flux cytometry

4T1 cell suspensions were incubated with a monoclonal rat anti-mouse CD9 conjugated to APC or a rat anti IgG_{2A} control isotype (R&D Systems). Analysis of CD9 cell surface production was performed using FACS Canto II and FACS Diva software (BD Biosciences).

Statistics

Results were presented as mean ± SEM. Statistical analyses were performed with GraphPad Prism version 5. Gaussian distribution was tested with Kolmogorov-Smirnov test, and a Student *t* test, an 1-way analysis of variance, a Mann-Whitney test, or a Kruskal-Wallis test was applied according to the sample distribution. Differences were considered as significant with *P* value less than .05.

Results

Neutrophil accumulation in premetastatic lung

To determine the precise timing of tumor cell dissemination to lungs in our experimental settings, tumor-bearing mice were killed at different time points (days 3, 7, 9, 14, and 21) after the subcutaneous injection of luciferase-expressing 4T1 cells (Figure 1A). Metastasis occurrence in lung tissues was revealed through bioluminescence imaging and histologic analyses. These later showed a positive bioluminescent signal and the presence of tumor islets on lung tissues sections only in lungs of mice 21 days after tumor cell injection (Figure 1B). To verify the sensitivity and specificity of our observations, the presence of tumor cells at early stages that could not be detected by bioluminescence or histologic studies was sought by performing primary cultures of cells issued from homogenized lung tissue. These cultures revealed the presence of tumor cells in lungs of mice bearing tumors in flanks, as early as 9 days after tumor cell implantation (Figure 1C). No tumor cell was, however, detected in primary cell cultures of lungs harvested 7 days after tumor cell inoculation in the subcutaneous tissues. These results prompted us to focus our subsequent analyses at this time point (day 7), which we considered as being a premetastatic stage. Consistent with the literature,[18,44] lungs of mice sacrificed at day 7 after subcutaneous tumor cell injection displayed several features of premetastatic niche including increased collagen cross-linking, LOX messenger RNA expression as well as enhanced MMP-2 and MMP-9 expression (Figures 1D to F). Furthermore, at day 7, neutrophil counts in bronchoalveolar

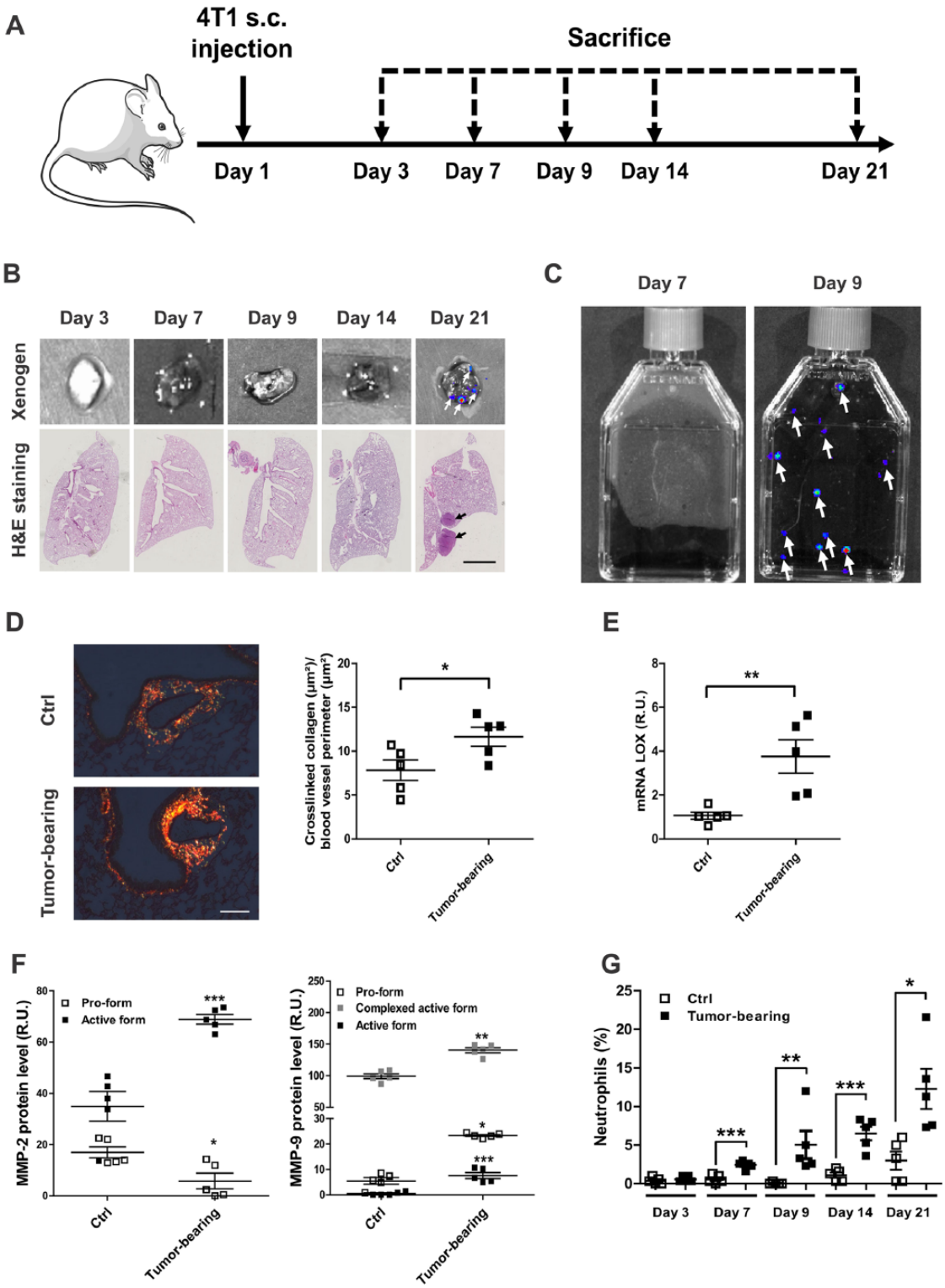

Figure 1. Neutrophils are recruited in premetastatic lungs corresponding to day 7 after the subcutaneous injection of 4T1 cells. (A) Schematic representation of the xenograft model protocol. Balb/C mice were subcutaneously injected with 4T1 cells (tumor-bearing) or medium alone (Ctrl). (B) Representative Xenogen IVIS and histologic analyses of lungs of mice sacrificed at days 3, 7, 9, 14, and 21 after subcutaneous injections of 4T1 tumor cells. Scale bar represents 2,5 mm. (C) Representative Xenogen IVIS analysis of lung primary cultures obtained from tumor-bearing mice sacrificed on days 7 and 9 following the primary tumor implantation. (D) Analysis of cross-linked collagen stained with picro-red staining in tumor-bearing and corresponding control lungs. Results are expressed in mean ± SEM, $^{*}P < .05$, Student *t* test (n = 5). (E) LOX messenger RNA expression in tumor-bearing (n = 5) and control lungs evaluated by reverse transcription-polymerase chain reaction. Results are expressed in mean ± SEM, $^{*}P < .05$; Student *t* test (n = 5). (F) Analysis of gelatinase production by zymography. Results are expressed as mean ± SEM, $^{*}P < .05$, $^{**}P < .01$, $^{***}P < .001$; Student *t* test. (G) Neutrophil counts in bronchoalveolar lavage (BAL) presented as the percentage within 300 cells in BAL of mice. Results are expressed as mean ± SEM. $^{*}P < .05$, $^{**}P < .01$, $^{***}P < .001$; Student *t* test (n = 5).

lavage (BAL) were increased in tumor-bearing mice as compared with control mice. The neutrophilic inflammation progressively increased from day 7 to day 21 (Figure 1G).

Increase in IL-16 expression in lungs displaying a premetastatic stage

A chemokine array performed on homogenized lung tissues showed increased levels of IL-16 in premetastatic lungs compared with control lungs (Figure 2A). Enzyme-linked immunosorbent assay and Western blot analyses confirmed increased levels in the premetastatic lung homogenates (Figures 2B to C), whereas IL-16 levels were similar in serum samples and BAL fluids (BALF) (Figures 2D to E). An immunohistochemistry targeting IL-16 revealed that cells producing IL-16 present in the premetastatic lungs and those cells are clearly are present in the lung parenchyma later during metastasis development (Figure 2F). Interestingly, 4T1 cells do not produce IL-16 as proven by IL-16 measurement in medium conditioned by 4T1 cells (data not shown). These data therefore demonstrate that, in our experimental settings, IL-16 is not released by tumor cells but rather by cells derived from the premetastatic lung microenvironment.

Neutrophils recruited in the premetastatic lungs produce IL-16

To evaluate whether neutrophils could be a source of IL-16 in the pulmonary parenchyma at a premetastatic stage, immunofluorescence studies were performed and revealed a colocalization between neutrophils and IL-16 in premetastatic lung tissues (Figure 3A). Lung neutrophils were next isolated by magnetic-activated cell sorting (MACS) and studied *in vitro* (Figures 3B to C). Unstimulated neutrophils sorted from lungs of mice bearing 4T1 primary tumors secreted detectable amounts of IL-16 in culture supernatant (Figure 3D). Interestingly, *in vitro* treatment of those cultured neutrophils with medium conditioned by 4T1 cells stimulated a IL-16 release by neutrophils (Figure 3D). Moreover, neutrophil depletion in lungs at a premetastatic stage using a blocking anti-Ly6G antibody resulted in a significant decrease in IL-16 lung levels (Figures 3E to F). These data suggest that 4T1 cell–derived soluble factors induce the secretion of IL-16 by neutrophils.

Microenvironment of premetastatic lungs displays increased expression of IL-16 in response to 4T1-derived signals

To determine the mechanisms involved in 4T1 cell metastasis development in lungs, naive mice were instilled with 4T1-conditioned medium or control medium. Protein extracts from lungs of mice treated with 4T1-conditioned medium displayed increased levels of IL-16 as compared with control mice (Figure 4A). In parallel, BAL differential cell counts showed that mice treated with 4T1-conditioned medium display higher neutrophil counts (Figure 4B). Enzyme-linked immunosorbent assay experiments performed on 4T1-conditioned medium revealed that tumor cells are able to produce several factors acting on neutrophil behavior such as KC (3979 ± 74.33 pg/mL), s100A8 (234.5 ± 89.46 pg/mL), and granulocyte-macrophage colony-stimulating factor (GM-CSF) (77.07 ± 1.77 pg/mL). Finally, instillations of 4T1-conditioned medium increased the ingression of metastatic cells into lung parenchyma after an intravenous injection of 4T1 cells (Figures 4C to D).

IL-16 contributes to the establishment of lung metastasis

To evaluate IL-16 implication in the metastatic process, an anti-IL-16 blocking antibody was instilled in mice bearing subcutaneous tumors in their flanks on days 7, 11, 15, and 19 following the tumor cell injection (Figure 5A). This treatment did not affect the primary tumor development because similar tumor volumes and weights were measured in control isotype-treated and antibody-treated mice (Figure 5B). In sharp contrast, the extent of metastatic dissemination in lung parenchyma was reduced in mice treated with anti-IL-16 antibody as shown by biophotonic imaging (IVIS) and histologic quantification (Figures 5C to D).

IL-16 influences tumor cell behavior in vitro

To assess whether IL-16 influences tumor cell behavior *in vitro*, an adhesion assay was first performed, in which 4T1 cells pretreated with a CellTracker Green were cultured with increase concentrations of a recombinant IL-16 on a murine endothelial SVEC 4.10 cell monolayer. Cell adhesiveness was measured after 45 minutes and showed that 4T1 cells displayed an increased adhesiveness to the murine endothelial SVEC 4.10 cell monolayer in a dose-dependent manner (1-20 ng/mL) (Figures 6A to C). In a scratch assay and an invasion assay using Matrigel-coated Boyden chambers, IL-16–stimulated 4T1 cell migration (Figures 6D to E), and invasion (Figures 6F to G), respectively. Recombinant IL-16 was not able to attract 4T1 cells in a Boyden chamber assay and did not modify tumor cell proliferation in a BrdU assay (data not shown).

CD9 has been reported as a cell surface receptor for IL-16.[23] Interestingly, CD9 was found to be expressed at 4T1 cell surface (Figure 6H) suggesting that IL-16–induced modulations might be induced by an interaction with CD9 at the surface of 4T1 cells.

Discussion

In this study, we assign a novel function to neutrophil-derived IL-16 during the elaboration of a premetastatic niche in lung parenchyma. This is supported by (1) the increased IL-16

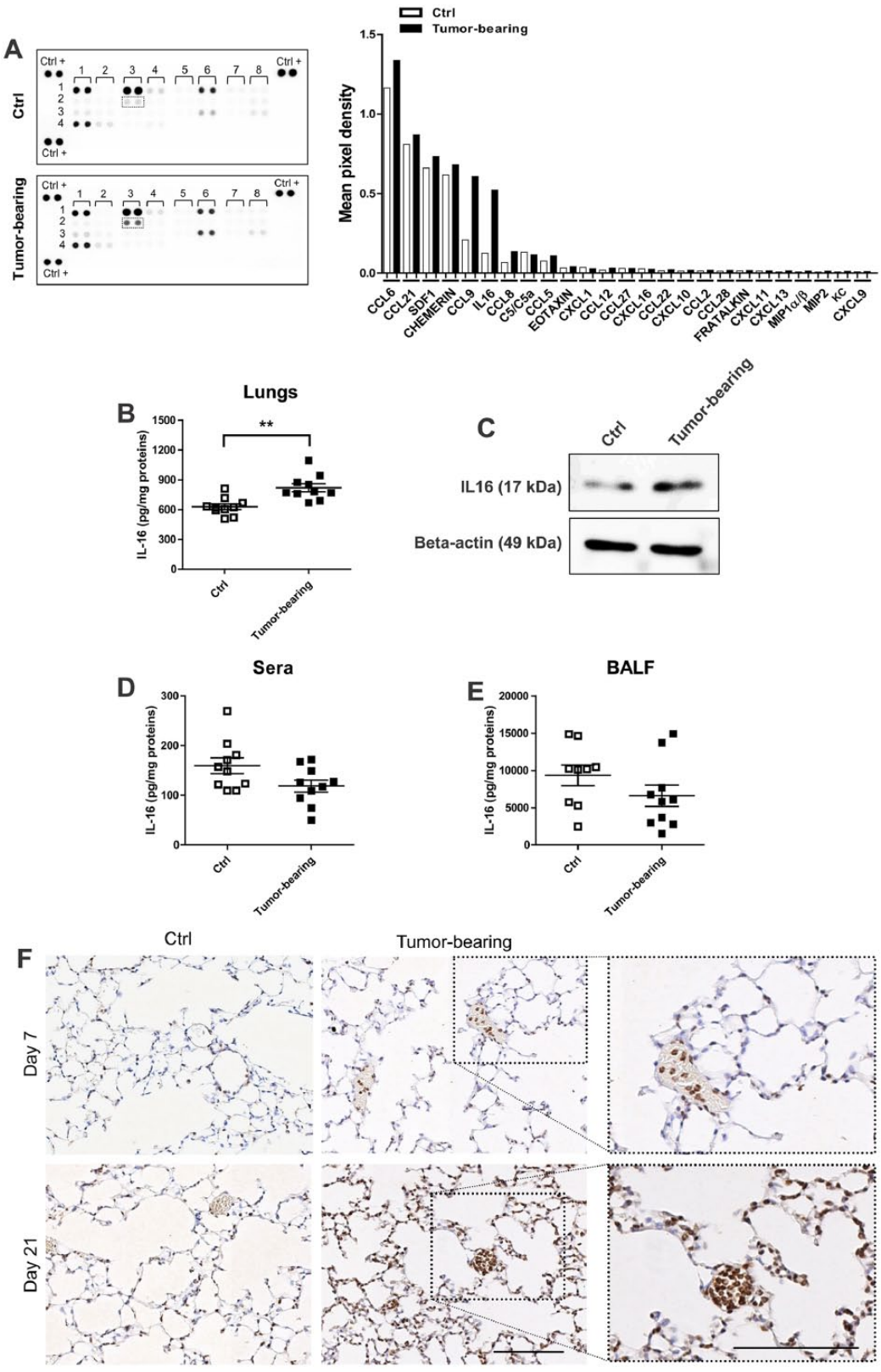

Figure 2. IL-16 level is increased in lungs at a premetastatic stage. (A) Chemokine array performed on pooled total protein extracts obtained from premetastatic and control lungs (n = 5) and dot quantification (right panel). (B) IL-16 measurement by ELISA performed on lungs protein extracts. (C) Representative Western blot of secreted IL-16 production at day 7 in lungs of tumor-bearing or control mice (blot performed on pooled total protein extracts obtained, n = 9-10). Actin serves as a loading control. ELISA anti-IL-16 performed on (D) serum samples and (E) bronchoalveolar lavage fluids obtained from tumor-bearing mice or control mice at day 7. Results are expressed as mean ± SEM. $^{**}P < .01$, Student *t* test (n = 10). (F) Representative immunohistochemistry against IL-16 performed on lung sections obtained from tumor-bearing and control mice sacrificed at days 7 and 21 following the primary tumor implantation. Scale bar represents 200 µm. ELISA indicates enzyme-linked immunosorbent assay; IL-16, interleukin 16.

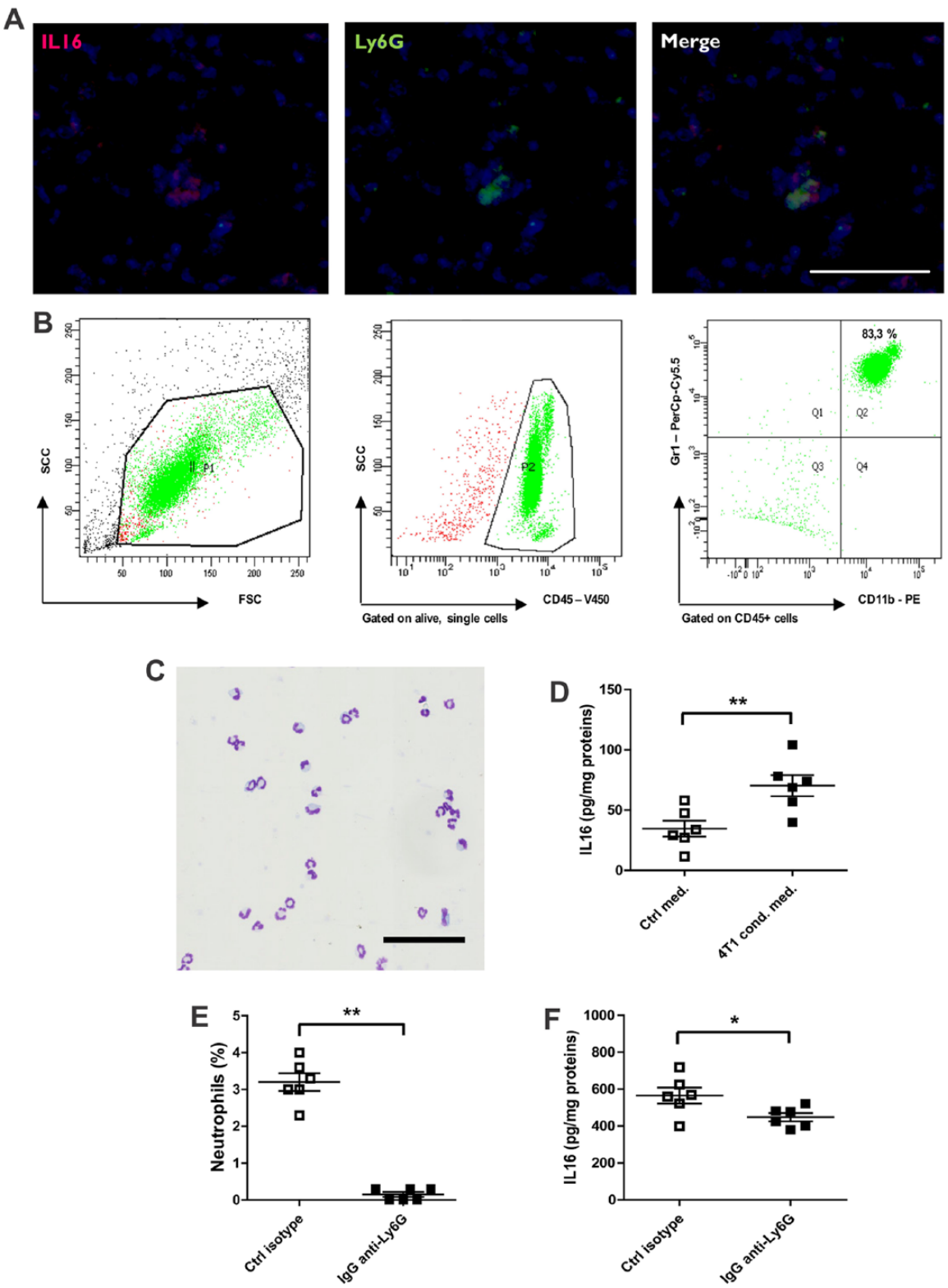

Figure 3. Neutrophils expressed IL-16 in premetastatic lungs. (A) Representative immunofluorescence experiments showing a colocalization between neutrophil foci and IL-16–positive area in premetastatic lungs. Scale bar corresponds to 100 µm. (B) Representative flow cytometry plots showing the purity of neutrophil isolation by MACS technologies. (C) Representative cytocentrifugation of neutrophils obtained using MACS technologies. Scale bar represents 100 µm. (D) IL-16 dosage by enzyme-linked immunosorbent assay in culture supernatant of neutrophils treated or not with 4T1-conditioned medium. Results are expressed as mean ± SEM. $^{**}P < .01$, Student *t* test. (E) Neutrophil percentage in bronchoalveolar lavage of tumor-bearing mice treated with a Ly6G blocking antibody or a control isotype. Results are expressed as mean ± SEM. $^{**}P < .01$, Mann-Whitney test (n = 6). (F) IL-16 dosage in lungs of tumor-bearing mice treated with a Ly6G blocking antibody or a control isotype. Results are expressed as mean ± SEM. $^{*}P < .05$, Student *t* test (n = 6). IL-16 indicates interleukin 16; MACS, magnetic-activated cell sorting.

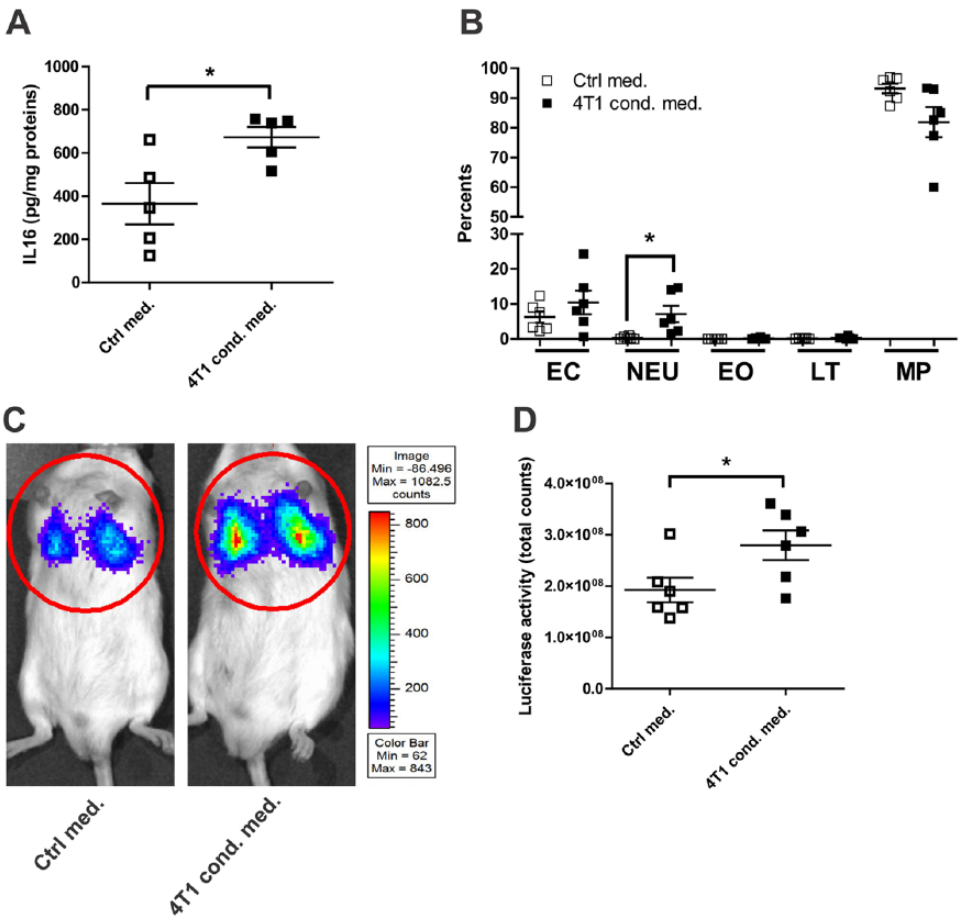

Figure 4. Soluble factors derived from 4T1 cells induced IL-16 production in the pulmonary microenvironment. (A) ELISA against IL-16 on whole lung protein homogenates obtained from mice intratracheally instilled with control medium or 4T1-conditioned medium. Results are expressed as mean ± SEM. *$P < .05$, Mann-Whitney test (n = 6). (B) Percentage of cell content in BAL of mice intratracheally instilled with control medium or 4T1-conditioned medium (EC: epithelial cells, NEU: neutrophils, EO: eosinophils, LT: lymphocytes, and MP: macrophages). Results are expressed in mean ± SEM. *$P < .05$, Student *t* test (n = 6). (C) Representative Xenogen IVIS analysis and bioluminescence quantification of lungs obtained from mice treated with control medium or 4T1-conditioned medium and receiving an intravenous injection of 4T1 cell. Results are expressed as mean ± SEM. *$P < .05$, Student *t* test (n = 6). IL-16 indicates interleukin 16.

levels (more than 4 times vs controls) in lung parenchyma at a premetastatic stage, (2) the decrease in lung metastasis when IL-16 is blocked, and (3) the ability of IL-16 to significantly modify 4T1 cell adhesion, migration, and invasiveness. These findings strongly advocate for a key role of IL-16 that is also supported by preclinical and clinical observations. Indeed, IL-16 is associated with primary tumor progression of breast cancer in preclinical models.[37] In humans, high IL-16 serum levels have been correlated with a poorer prognosis in metastatic cancers (eg, breast, myeloma, gastrointestinal, ovarian, and renal cancers),[32] and IL-16 gene polymorphisms are associated with the susceptibility to develop primary cancers (eg, colorectal, gastric, and renal cancers).[33,35,45,46] To date, a relationship between IL-16 and metastases has not been reported. To unveil the mechanisms linking IL-16 upregulation and cancer progression, we explored the potential role of IL-16 in the premetastatic niche. The originality of this work is to demonstrate that this cytokine plays a role in early steps of the lung metastasis process.

We chose to use an experimental 4T1 tumor xenograft model to study modulations occurring in the microenvironment before the arrival of metastatic cells (premetastatic niche) because those cells have a high metastatic potential[47] and are considered to mimic some aspects of breast cancer dissemination.[38,47,48] One of the main challenges in studying premetastatic niches is to determine the timing of organ colonization by tumor cells. As other authors showed that 4T1 tumor already metastasizes to lungs and liver from day 8 posttransplantation,[49] we performed clonogenic metastasis assays on digested lungs after several durations of primary tumor implantation as described by DuPré et al,[38] and we concomitantly analyzed premetastatic niche characteristics as described by Erler et al.[18] This protocol allowed us to confirm that day 7 following 4T1 cell transplantation corresponds to a premetastatic stage and this is in accordance with previous reports.[15]

There is strong evidence that immune/inflammatory cells recruited in the target organ prior to tumor cell arrival play a key role in the metastasis process.[10–18] As an intact immune

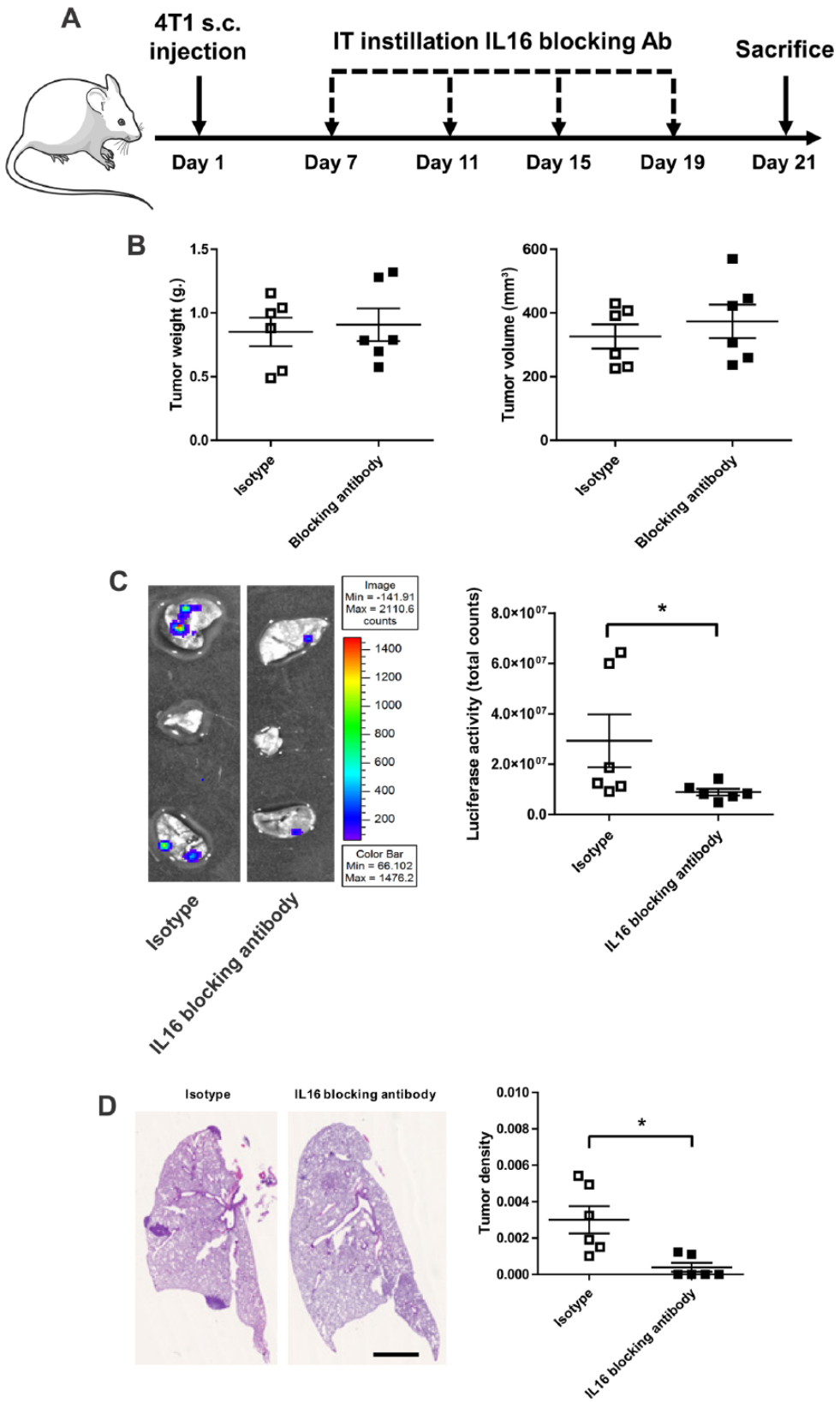

Figure 5. Impact of the IL-16 depletion on the pulmonary metastasis occurrence. (A) Schematic representation of the protocol for the IL-16 blocking antibody administration to tumor-bearing mice. (B) Comparison of the primary tumor weight (left panel) and volume (right panel) after administration of the IL-16 blocking antibody or a control isotype. Student t test (n=6). (C) Representative Xenogen IVIS analysis and bioluminescence quantification of lungs obtained from tumor-bearing mice treated with an IL-16 blocking antibody or a control isotype. Results are expressed in mean ± SEM. *$P < .05$, Mann-Whitney test (n = 6). (D) Representative histologic sections and tumor density quantification in lungs obtained from tumor-bearing mice treated with an IL-16 blocking antibody or a control isotype. Scale bar represents 2 mm. Results are expressed in mean ± SEM. *$P < .05$, Mann-Whitney test (n = 6). IL-16 indicates interleukin 16.

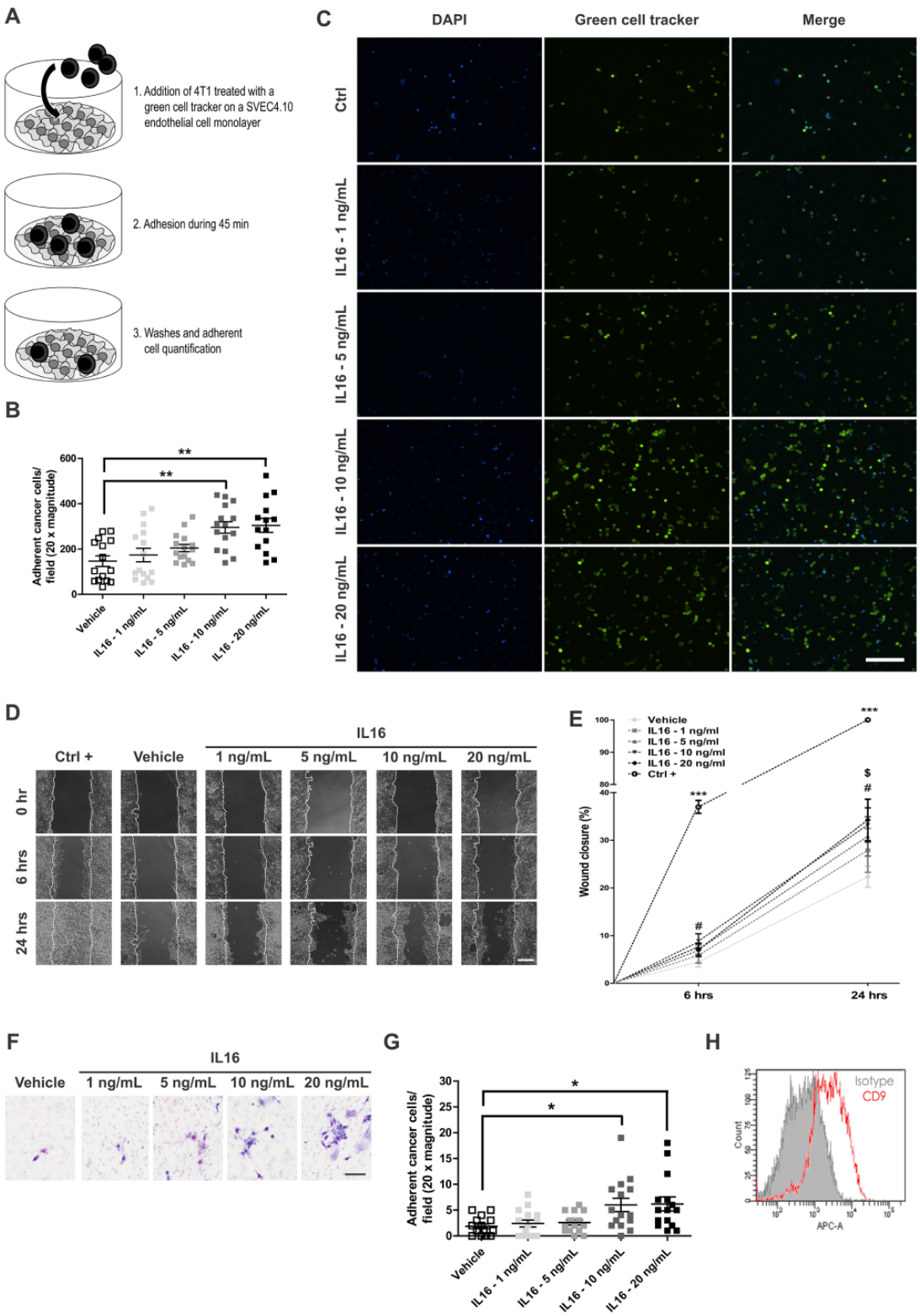

Figure 6. IL-16 improved the adhesion, migration and invasion of 4T1 cells. (A) Protocol for adhesion assay. (B) Impact of increasing concentrations of IL-16 on 4T1 cell adhesion on a confluent murine endothelial SVEC4.10 cell monolayer. Results are expressed as mean ± SEM. $^{**}P < .01$, Kruskal-Wallis test. (C) Representative pictures corresponding to each condition tested in the adhesion assay. Scale bar corresponds to 200 µm. (D) Representative pictures obtained by scratch assay. Scale bar corresponds to 200 µm. (E) Quantification of the effect of increasing concentrations of IL-16 on 4T1 cell migration evaluated by scratch assay. Ctrl+ condition corresponds to a 4T1 migration in presence of complete supplemented medium. Wound closure was expressed in percentage regarding the scratch area reported at the beginning of the experiment. Results are expressed in mean ± SEM. $^{\#}P < .05$ (vehicle vs IL-16, 10 ng/mL), $^{\$}P < .05$ (vehicle vs IL-16, 20 ng/mL), $^{***}P < .001$ (vehicle vs Ctrl+), 1-way ANOVA. (F) Representative pictures obtained for the invasion assay. Scale bar corresponds to 100 µm. (G) Quantification of the effect of increasing concentrations of IL-16 on 4T1 invasion across a Matrigel-coated insert. $^{*}P < .05$, 1-way ANOVA. (H) Expression of CD9 at the 4T1 cell surface evaluated by flux cytometry. ANOVA indicates analysis of variance; IL-16, interleukin 16.

system is mandatory to study the interactions between tumor cells, organs, and immune cells, we chose to use the 4T1 mammary cancer model. Indeed, 4T1 cells derive from a spontaneously arising mammary tumor in BALB/cfC3H mice[50] and the transplantation of 4T1 cells in syngenic mice allowed us to investigate the contribution of an intact immune system to the pulmonary premetastatic niche. Studying the role of neutrophils in premetastatic niches is of highest interest because (1) neutrophils are recruited in premetastatic lungs in breast cancer in *in vivo* models as shown in our study and previously reported by others[15–17] and (2) an accumulation of neutrophils has been reported in patients having breast cancer.[51,52] Nevertheless, there are controversies about the exact role of neutrophils in the metastatic process with authors reporting prometastatic roles,[53–55] whereas others report antimetastatic functions.[56] Similarly, the contribution of neutrophils to the premetastatic pulmonary niche is still controversial and mechanisms are still to be unveiled.[15–17] Granot et al.[15] showed that CCL2-entrained neutrophils inhibit lung metastasis by H_2O_2 production. However, Wculek et al.[16] more recently reported a prometastatic role of neutrophils through leukotriene production allowing a metastasis promotion by selectively expanding a subpool of cancer cells with high tumorigenic potential. Our results clearly indicate that neutrophils recruited to premetastatic lungs contribute to the development of lung metastasis by IL-16 production, suggesting a new mechanism of metastasis promotion. Subtle differences in experimental procedures might account for the differences between our results and those reported by Granot et al.[15] Indeed, the timing of neutrophil inhibition is different among studies. Here, we focused on the short term because our study was focused on the early steps of lung colonization. A recent study reported that neutrophil depletion at several phases of metastatic cascade in a breast cancer model decreases metastasis in the early phase but not the late phase.[57] Moreover, the anti-Ly6G antibody depleted all neutrophils including also those present in the primary tumor, implying that primary tumor profile could be altered. Indeed, neutrophils have been reported as participating to primary tumor progression and angiogenesis through the production of several factors (eg, MMP-9, oncostatin M, elastase, CXCL1, CXCL2, and IL6).[58–62] Thus, results of a long-term neutrophil depletion, such as described by Granot et al.,[15] regarding the metastasis development could be an indirect indicator of a primary tumor profile modulation. Another remarkable difference between our study and the results reported by Granot et al.[15] is that they performed *in vitro* assays using neutrophils isolated from blood circulation, whereas we focused our study on neutrophils purified from premetastatic lung parenchyma. This might account for most differences because subpopulations of neutrophils are likely to display very different characteristics that affect their activity against tumor cells. Indeed, neutrophil subtype appears to be microenvironment dependent[63] and circulating neutrophils are not embedded in the complex modified microenvironment of premetastatic lungs. Moreover, recent study described that circulating neutrophils with a high cytotoxic activity predominate in early steps of tumor development resulting in a global antitumor effect, whereas these cells display tumor-supporting capacities once tumor progresses.[64] Finally, immune cells that interfere with cancer progression are part of a complex network that is still not fully understood, and subtle experimental details might greatly affect the prometastatic or antimetastatic role of neutrophils. Nevertheless, these considerations do not modify our main conclusion that IL-16 plays a key role in the premetastatic niche. Interleukin 16 has already been reported as produced by neutrophils.[21] In this study, we clearly identified neutrophils as a main contributor of the IL-16 increase in the premetastatic lungs. This is supported by (1) immunofluorescence experiments showing a colocalization between neutrophils and IL-16 in the premetastatic lung parenchyma and (2) a significant IL-16 decrease in premetastatic lungs when neutrophils were depleted in tumor-bearing mice. However, IL-16 has been reported to be also produced by other cell type such as pulmonary epithelial cells,[65,66] eosinophils,[67] macrophages,[68] or mast cells.[69] Our experimental settings cannot rule out a potential partial contribution of these cell types to the IL-16 increase observed in the pulmonary parenchyma during the metastasis establishment time course. The exact molecular mechanisms underlying the IL-16–driven increased lung metastasis remains to be determined. Our *in vitro* data demonstrate that IL-16 contributes to an increased adhesiveness, migration, and invasiveness of 4T1 cells. In our experimental setting, CD9 was expressed by 4T1 tumor cells and might take part to a pathway including IL-16 and contribute to cancer dissemination. Indeed, CD9 is a receptor for IL-16,[23] and CD9 overexpression by MCF7 breast cancer cells promotes metastasis in experimental models.[70] Moreover, CD9 inhibition or knockdown was reported to suppress the metastatic capacity of different breast cancer cell lines through a decrease in invasiveness and migration of tumor cells.[71]

The mechanism of IL-16 induction by breast cancer cells in neutrophils is still to be determined. Nevertheless, we showed that 4T1 cells are able to produce s100A8, KC, and GM-CSF that were shown as be able to modulate neutrophil behavior (chemoattraction, survival, functional activation, etc).[72–74] S100A8 is particularly interesting because this molecule is overexpressed in the premetastatic niche[75] where it is produced by myeloid cells and pulmonary epithelium. Then, s100A8 and GM-CSF appeared to be able to stimulate neutrophils to produce IL-16 and could represent a link between 4T1 and neutrophil-derived IL-16 overexpression.[21] Further studies are needed to identify clearly the 4T1 cell-derived cytokine potentiating the IL-16 release from neutrophils.

Our study was focused on the effects of IL-16 on metastatic dissemination and our hypothesis is that IL-16 display a direct effect on tumor cells. However, we cannot rule out a potential

additional indirect effect of IL-16 on metastasis development by acting on the pulmonary microenvironment. Indeed, as the main function described for IL-16 is lymphocyte activation and recruitment,[19,20] IL-16 could recruit and influence the development of regulator T cells in the premetastatic stage as already described in asthma pathology.[76] Indeed, this cell type generally is considered to be a significant contributor to tumor escape from the host immune system and could improve the metastasis development in lungs.

In conclusion, this study demonstrates that IL-16 is a key mediator in premetastatic niches that drives the establishment of lung metastasis and might represent a suitable therapeutic target.

Acknowledgements

The authors thank Pascale Heneaux, Fabienne Perin, Céline Vanwinge, and Christine Fink for technical support. They also acknowledge the GIGA-Imaging and Flow Cytometry.

Author Contributions

KD contributed to conception and design of the work, data collection, analysis interpretation, preparation of figures, and manuscript preparation. CS contributed to data collection and interpretation of results and drafting of figures. NR contributed to data collection, interpretation of results, supervision of in vivo experiments, and critically revised the manuscript. SB did most of the images analysis and interpretation. CR contributed to data collection and interpretation of results. AN did take part to project supervision, contributed to manuscript preparation, and critically revised the manuscript. DC designed the project, conceived the research program, applied to grants for funding, supervised the project on a day-to-day basis, supervised manuscript preparation, approved the final version to be published, and submitted the manuscript to the editor.

Disclosures and Ethics

The experimental protocol for animal studies was examined and approved on December 12, 2012 by the Ethical Committee of the University of Liege and accepted under the reference number #1376.

REFERENCES

1. Chaffer CL, Weinberg RA. A perspective on cancer cell metastasis. *Science*. 2011;331:1559–1564.
2. Siegel RL, Miller KD, Jemal A. Cancer statistics, 2016. *CA Cancer J Clin*. 2016;66:7–30.
3. Giordano SH, Buzdar AU, Smith TL, Kau S-W, Yang Y, Hortobagyi GN. Is breast cancer survival improving? *Cancer*. 2004;100:44–52.
4. Lobbezoo DJA, van Kampen RJW, Voogd AC, et al. Prognosis of metastatic breast cancer: are there differences between patients with de novo and recurrent metastatic breast cancer? *Br J Cancer*. 2015;112:1445–1451.
5. Paget S. The distribution of secondary growths in cancer of the breast. *Lancet*. 1889;133:571–573.
6. Weigelt B, Peterse JL, Van Veer LJ. Breast cancer metastasis: markers and models. *Nat Rev Cancer*. 2005;5:591–602.
7. Kaplan RN, Psaila B, Lyden D. Bone marrow cells in the "pre-metastatic niche": within bone and beyond. *Cancer Metastasis Rev*. 2006;25:521–529.
8. Psaila B, Kaplan RN, Port ER, Lyden D. Priming the "soil" for breast cancer metastasis: the pre-metastatic niche. *Breast Dis*. 2007;26:65–74.
9. Sceneay J, Smyth MJ, Möller A. The pre-metastatic niche: finding common ground. *Cancer Metastasis Rev*. 2013;32:449–464.
10. Kaplan RN, Riba RD, Zacharoulis S, et al. VEGFR1-positive haematopoietic bone marrow progenitors initiate the pre-metastatic niche. *Nature*. 2005;438:820–827.
11. Gao D, Joshi N, Choi H, et al. Myeloid progenitor cells in the premetastatic lung promote metastases by inducing mesenchymal to epithelial transition. *Cancer Res*. 2012;72:1384–1395.
12. Kitamura T, Qian B, Pollard JW. Immune cell promotion of metastasis. *Nat Publ Gr*. 2015;15:73–86.
13. Sceneay J, Chow MT, Chen A, et al. Primary tumor hypoxia recruits CD11b+/Ly6Cmed/Ly6G+ immune suppressor cells and compromises NK cell cytotoxicity in the premetastatic niche. *Cancer Res*. 2012;72:3906–3911.
14. Sharma SK, Chintala NK, Vadrevu SK, Patel J, Karbowniczek M, Markiewski MM. Pulmonary alveolar macrophages contribute to the premetastatic niche by suppressing antitumor T cell responses in the lungs. *J Immunol*. 2015;194:5529–5538.
15. Granot Z, Henke E, Comen EA, King TA, Norton L, Benezra R. Tumor entrained neutrophils inhibit seeding in the premetastatic lung. *Cancer Cell*. 2011;20:300–314.
16. Wculek SK, Malanchi I. Neutrophils support lung colonization of metastasis-initiating breast cancer cells. *Nature*. 2015;528:413–417.
17. Wu CF, Andzinski L, Kasnitz N, et al. The lack of type I interferon induces neutrophil-mediated pre-metastatic niche formation in the mouse lung. *Int J Cancer*. 2015;847:837–847.
18. Erler JT, Bennewith KL, Cox TR, et al. Hypoxia-induced lysyl oxidase is a critical mediator of bone marrow cell recruitment to form the premetastatic niche. *Cancer Cell*. 2009;15:35–44.
19. Cruikshank W, Center DM. Modulation of lymphocyte migration by human lymphokines. II. Purification of a lymphotactic factor (LCF). *J Immunol*. 1982;128:2569–2574.
20. Richmond J, Tuzova M, Cruikshank W, Center D. Regulation of cellular processes by interleukin-16 in homeostasis and cancer. *J Cell Physiol*. 2014;229:139–147.
21. Katano M, Okamoto K, Suematsu N, et al. Increased expression of S1OO calcium binding protein A8 in GM-CSF-stimulated neutrophils leads to the increased expressions of IL-8 and IL-16. *Clin Exp Rheumatol*. 2011;29:768–775.
22. Center DM, Kornfeld H, Cruikshank WW. Interleukin 16 and its function as a CD4 ligand. *Immunol Today*. 1996;17:476–481.
23. Qi JC, Wang J, Mandadi S, et al. Human and mouse mast cells use the tetraspanin CD9 as an alternate interleukin-16 receptor. *Blood*. 2006;107:135–142.
24. Bowler RP, Bahr TM, Hughes G, et al. Integrative omics approach identifies interleukin-16 as a biomarker of emphysema. *OMICS*. 2013;17:619–626.
25. Cho M-L, Jung YO, Kim K-W, et al. IL-17 induces the production of IL-16 in rheumatoid arthritis. *Exp Mol Med*. 2008;40:237–245.
26. Middel P, Reich K, Polzien F, et al. Interleukin 16 expression and phenotype of interleukin 16 producing cells in Crohn's disease. *Gut*. 2001;49:795–803.
27. Burkart KM, Barton SJ, Holloway JW, et al. Association of asthma with a functional promoter polymorphism in the IL16 gene. *J Allergy Clin Immunol*. 2006;117:86–91.
28. Pinsonneault S, El Bassam S, Mazer B, Cruikshank WW, Laberge S. IL-16 inhibits IL-5 production by antigen-stimulated T cells in atopic subjects. *J Allergy Clin Immunol*. 2001;107:477–482.
29. Hessel EM, Cruikshank WW, Van Ark I, et al. Involvement of IL-16 in the induction of airway hyper-responsiveness and up-regulation of IgE in a murine model of allergic asthma. *J Immunol*. 1998;160:2998–3005.
30. Cruikshank WW, Long A, Tarpy RE, et al. Early identification of interleukin-16 (lymphocyte chemoattractant factor) and macrophage inflammatory protein 1 alpha (MIP1 alpha) in bronchoalveolar lavage fluid of antigen-challenged asthmatics. *Am J Respir Cell Mol Biol*. 1995;13:738–747.
31. Alexandrakis MG, Passam FH, Kyriakou DS, et al. Serum level of interleukin-16 in multiple myeloma patients and its relationship to disease activity. *Am J Hematol*. 2004;75:101–106.
32. Kovacs E. The serum levels of IL-12 and IL-16 in cancer patients. Relation to the tumour stage and previous therapy. *Biomed Pharmacother*. 2001;55:111–116.
33. Gao LB, Rao L, Wang YY, et al. The association of interleukin-16 polymorphisms with IL-16 serum levels and risk of colorectal and gastric cancer. *Carcinogenesis*. 2009;30:295–299.
34. Yellapa A, Bitterman P, Sharma S, et al. Interleukin 16 expression changes in association with ovarian malignant transformation. *Am J Obstet Gynecol*. 2014;210:272.e1-272.e10.
35. Batai K, Shah E, Murphy AB, et al. Fine-mapping of IL16 gene and prostate cancer risk in African Americans. *Cancer Epidemiol Biomarkers Prev*. 2012;21:2059–2068.

36. Compérat E, Rouprêt M, Drouin SJ, et al. Tissue expression of IL16 in prostate cancer and its association with recurrence after radical prostatectomy. *Prostate*. 2010;70:1622–1627.
37. Milke L, Schulz K, Weigert A, Sha W, Schmid T, Brüne B. Depletion of tristetraprolin in breast cancer cells increases interleukin-16 expression and promotes tumor infiltration with monocytes/macrophages. *Carcinogenesis*. 2013;34:850–857.
38. DuPré SA, Redelman D, Hunter KW. The mouse mammary carcinoma 4T1: characterization of the cellular landscape of primary tumours and metastatic tumour foci. *Int J Exp Pathol*. 2007;88:351–360.
39. Cataldo D, Munaut C, Noël A, et al. MMP-2- and MMP-9-linked gelatinolytic activity in the sputum from patients with asthma and chronic obstructive pulmonary disease. *Int Arch Allergy Immunol*. 2000;123:259–267.
40. Keane J, Nicoll J, Kim S, et al. Conservation of structure and function between human and murine IL-16. *J Immunol*. 1998;160:5945–5954.
41. Meagher C, Beilke J, Arreaza G, et al. Neutralization of interleukin-16 protects nonobese diabetic mice from autoimmune type 1 diabetes by a CCL4-dependent mechanism. *Diabetes*. 2010;59:2862–2871.
42. Yoshimoto T, Wang CR, Yoneto T, Matsuzawa A, Cruikshank WW, Nariuchi H. Role of IL-16 in delayed-type hypersensitivity reaction. *Blood*. 2000;95:2869–2874.
43. Kleinman HK, Martin GR. Matrigel: basement membrane matrix with biological activity. *Semin Cancer Biol*. 2005;15:378–386.
44. Mauti LA, Le Bitoux MA, Baumer K, et al. Myeloid-derived suppressor cells are implicated in regulating permissiveness for tumor metastasis during mouse gestation. *J Clin Invest*. 2011;121:2794–2807.
45. Zhu J, Qin C, Yan F, et al. IL16 polymorphism and risk of renal cell carcinoma: association in a Chinese population. *Int J Urol*. 2010;17:700–707.
46. Qin X, Peng Q , Lao X, et al. The association of interleukin-16 gene polymorphisms with IL-16 serum levels and risk of nasopharyngeal carcinoma in a Chinese population. *Tumor Biol*. 2014;35:1917–1924.
47. Heppner GH, Miller FR, Shekhar PVM. Nontransgenic models of breast cancer. *Breast Cancer Res*. 2000;2:331–334.
48. Fantozzi A, Christofori G. Mouse models of breast cancer metastasis. *Breast Cancer Res*. 2006;8:212. Available at: http://breast-cancer-research.com/content/8/4/212
49. Kershaw MH, Jackson JT, Haynes NM, et al. Gene-engineered T cells as a superior adjuvant therapy for metastatic cancer. *J Immunol*. 2004;173:2143–2150.
50. Heppner GH, Dexter DL, Denucci T, Miller FR, Calabresi P. Heterogeneity in drug sensitivity among tumor cell subpopulations single mammary tumor. *Cancer Res*. 1978;38:3758–3763.
51. Azab B, Shah N, Radbel J, et al. Pretreatment neutrophil/lymphocyte ratio is superior to platelet/lymphocyte ratio as a predictor of long-term mortality in breast cancer patients. *Med Oncol*. 2013;30:432.
52. Noh H, Eomm M, Han A. Breast cancer usefulness of pretreatment neutrophil to lymphocyte ratio in predicting disease-specific survival in breast cancer patients. *J Breast Cancer*. 2013;16:55–59.
53. Nozawa H, Chiu C, Hanahan D. Infiltrating neutrophils mediate the initial angiogenic switch in a mouse model of multistage carcinogenesis. *PNAS*. 2006;103:12493–12498.
54. Tao L, Zhang L, Peng Y, Tao M, Li L, Xiu D. Neutrophils assist the metastasis of circulating tumor cells in pancreatic ductal adenocarcinoma. *Medicine*. 2016;95:e4932.
55. Gordon-Weeks AN, Lim SY, Yuzhalin AE, et al. Neutrophils promote hepatic metastasis growth through fibroblast growth factor 2-dependent angiogenesis in mice. *Hepatology*. 2017;65:1920–1935.
56. Hicks AM, Riedlinger G, Willingham MC, et al. Transferable anticancer innate immunity in spontaneous regression/complete resistance mice. *PNAS*. 2006;103:7753–7758.
57. Coffelt SB, Wellenstein MD, De Visser KE. Neutrophils in cancer: neutral no more. *Nat Rev Cancer*. 2016;16:431–446.
58. Houghton AM, Rzymkiewicz DM, Ji H, et al. Neutrophil elastase-mediated degradation of IRS-1 accelerates lung tumor growth. *Nat Med*. 2010;16:219–223.
59. Queen MM, Ryan RE, Holzer RG, Keller-Peck CR, Jorcyk CL. Breast cancer cells stimulate neutrophils to produce oncostatin M: potential implications for tumor progression. *Cancer Res*. 2005;65:8896–8905.
60. Ardi VC, Kupriyanova TA, Deryugina EI, Quigley JP. Human neutrophils uniquely release TIMP-free MMP-9 to provide a potent catalytic stimulator of angiogenesis. *Proc Natl Acad Sci U S A*. 2007;104:20262–20267.
61. Liang W, Ferrara N. The complex role of neutrophils in tumor angiogenesis and metastasis. *Cancer Immunol Res*. 2016;4:83–92.
62. Borregaard N, Sørensen OE, Theilgaard-Mönch K. Neutrophil granules: a library of innate immunity proteins. *Trends Immunol*. 2007;28:340–345.
63. Fridlender ZG, Sun J, Kim S, et al. Polarization of tumor-associated neutrophil (TAN) phenotype by TGF-β: "N1" versus "N2" TAN. *Cancer Cel*. 2010;16:183–194.
64. Sagiv JY, Michaeli J, Fridlender ZG, et al. Phenotypic diversity and plasticity in circulating neutrophil subpopulations in cancer. *Cell Rep*. 2015;10:562–573.
65. Little FF, Lynch E, Fine G, Center DM, Cruikshank WW. Tumor necrosis factor-α-induced synthesis of interleukin-16 in airway epithelial cells: priming for serotonin stimulation. *Am J Respir Cell Mol Biol*. 2003;28:354–362.
66. Yadav S, Shi Y, Wang H. IL-16 effects on A549 lung epithelial cells: dependence on CD9 as an IL-16 receptor? *J Immunotoxicol*. 2010;7:183–193.
67. Lim KG, Wan HC, Bozza PT, et al. Human eosinophils elaborate the lymphocyte chemoattractants. IL-16 (lymphocyte chemoattractant factor) and RANTES. *J Immunol*. 1996;156:2566–2570.
68. Liebrich M, Guo LH, Schluesener HJ, et al. Expression of interleukin-16 by tumor-associated macrophages/activated microglia in high-grade astrocytic brain tumors. *Arch Immunol Ther Exp (Warsz)*. 2007;55:41–47.
69. Rumsaeng V, Cruikshank WW, Foster B, et al. Human mast cells produce the CD4+ T lymphocyte chemoattractant factor, IL-16. *J Immunol*. 1997;159:2904–2910.
70. Kischel P, Bellahcene A, Deux B, et al. Overexpression of CD9 in human breast cancer cells promotes the development of bone metastases. *Anticancer Res*. 2012;32:5211–5220.
71. Rappa G, Green TM, Karbanová J, Corbeil D, Lorico A. Tetraspanin CD9 determines invasiveness and tumorigenicity of human breast cancer cells. *Oncotarget*. 2015;6:7970–7991.
72. Ritzman AM, Hughes-Hanks JM, Blaho VA, Wax LE, Mitchell WJ, Brown CR. The chemokine receptor CXCR2 ligand KC (CXCL1) mediates neutrophil recruitment and is critical for development of experimental lyme arthritis and carditis. *Infect Immun*. 2010;78:4593–4600.
73. Gomez-Cambronero J, Horn J, Paul CC, Baumann MA. Granulocyte-macrophage colony-stimulating factor is a chemoattractant cytokine for human neutrophils: involvement of the ribosomal p70 S6 kinase signaling pathway. *J Immunol*. 2003;171:6846–6855.
74. Zahran N, Sayed A, William I, Mahmoud O, Sabry O, Rafaat M. Neutrophil apoptosis: impact of granulocyte macrophage colony stimulating factor on cell survival and viability in chronic kidney disease and hemodialysis patients. *Arch Med Sci*. 2013;9:984–989.
75. Rafii S, Lyden D. S100 chemokines mediate bookmarking of premetastatic niches. *Nat Cell Biol*. 2006;8:1321–1323.
76. McFadden C, Morgan R, Rahangdale S, et al. Preferential migration of T regulatory cells induced by IL-16. *J Immunol*. 2007;179:6439–6445.